CHEMISTRY OF MATERIALS

ARTICLE

pubs.acs.org/cm

Incarceration of Nanosized Silica into Porous Coordination Polymers: Preparation, Characterization, and Adsorption Property

Takashi Uemura,*[,†] Yu Kadowaki,[†] Cho Rong Kim,[†] Tomohiro Fukushima,[†] Daisuke Hiramatsu,[†] and Susumu Kitagawa*[,†,‡]

[†]Department of Synthetic Chemistry and Biological Chemistry, Graduate School of Engineering, Kyoto University, Katsura, Nishikyo-ku, Kyoto 615-8510, Japan

[‡]Institute for Integrated Cell-Material Sciences (iCeMS), Kyoto University, Yoshida, Sakyo-ku, Kyoto 606-8501, Japan

ABSTRACT: Sol−gel polycondensation of tetramethoxysilane was performed in nanochannels of porous coordination polymers (PCPs), resulting in the formation of nanosized silica dispersed homogeneously inside the channels. In this system, the growth of silica was highly constrained, which increases the hydrophilic silanol moieties on the surface of silica particles. Deposition of silica particles into the nanochannels of PCPs could allow the remarkable alternations of the porous properties of the PCPs. Compared to the original PCP systems, adsorption of water was greatly enhanced because of the strong interaction between silica and water. The PCP−silica nanocomposites preferred to adsorb 1,4-dioxane rather than cyclohexane, showing the remarkable affinity of PCP−silica hybrids to hydrophilic molecules. It is noteworthy that pore dimensionality of PCPs have large effects on the adsorption properties of PCP−silica hybrids. Compared to a PCP with three-dimensional interconnecting nanochannels, a PCP with one-dimensional porous system showed more significant gate effects on selectivity for the adsorbates.

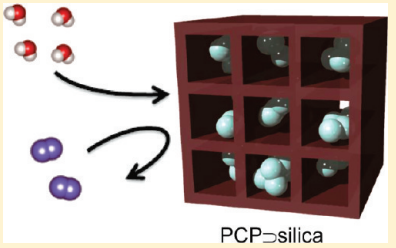

KEYWORDS: porous coordination polymers, silica, nanocomposites, adsorption property

INTRODUCTION

The design and synthesis of porous coordination polymers (PCPs) with unique structural topologies and electronic functions using self-assembly approach of metal ions and organic ligands have been the focus of intense activity.[1] Because of their ordered porous structures with a large surface area, permanent porosity, and surface functionality, PCPs have emerged as an important new class of nanoporous materials with potential for the many applications in storage, separation, catalysis, and chemical sensing.[1] To enhance these porous properties of PCP, deposition of inorganic particles (metal, metal oxide, and metal sulfide) into the nanochannels of PCPs has recently attracted much attention.[2] Fabrication of the host−guest nanocomposites between PCPs and inorganic particles has made rapid progress because doping of only small amount of the inorganic materials allows the remarkable alternations of the properties of PCPs. This methodology is useful enough to afford new functions to PCPs without changing the pore size, shape, and surface. For example, loading of PCPs with a variety of metal nanoparticles can allow catalytic properties for alcohol oxidation,[2b] hydrogenations,[2a,b,h] and Heck reaction.[2e] Encapsulation of Pd particles in PCP pores can enhance the adsorption property for hydrogen molecule.[2f,h]

Silica nanoparticles and nanostructures provide unprecedented material platforms to accomplish many nanoscale functions.[3] Many of the advances in silica nanochemistry are based on its transparency, stability, dielectric properties, and opportunities for introducing multiple functionalities. In particular, silanol moieties on the silica surface greatly contribute to the hydrophilic property of silica,[4] where the number of surface silanols increases with decreasing the size of silica. Thus, nanosized silica with large surface area will give remarkable effects on the adsorption behaviors after the formation of nanocomposite with host materials.

In a previous paper, we have reported the sol−gel synthesis of silica in one-dimensional channels of $[Cu_2(pzdc)_2(dpe)]_n$ (**CPL5**; pzdc = pyrazine-2,3-dicarboxylate, dpe =1,2-di(4-pyridyl)ethylene; pore size =10 × 6 Å^2, Figure 1).[2d] Although a few properties originated from the low dimensional silica were reported, unique functions derived from the formation of PCP−silica nanocomposites has not been investigated yet. In this work, we newly prepared a PCP−silica nanocomposite utilizing $[Cu_3(btc)_2]_n$with three-dimensional interconnecting nanochannels (**HKUST**; btc = benzene-1,3,5-tricarboxylate, pore size = 9 × 9 Å^2, Figure 1), and demonstrate that modification of PCP pores with nanosized silica remarkably enhances the porous properties of PCPs. It is noteworthy that hydrophilic molecules can be selectively adsorbed in the pores of the composites because of the strong interaction between the doped silica and the adsorbates. By comparison between the results obtained from **CPL5** and **HKUST**, we could understand that the dimensionality of PCP pores essentially affects the adsorption properties of PCP−silica composites.

Received: September 11, 2010
Revised: December 16, 2010
Published: March 09, 2011

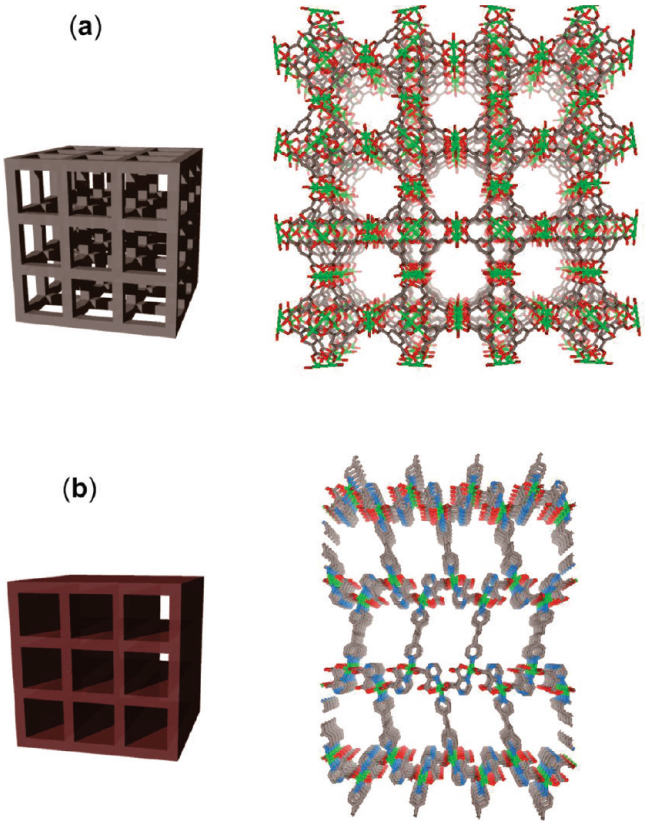

Figure 1. Nanochannel structures of (a) **HKUST** and (b) **CPL5** displayed by stick model (Cu, green; O, red; N, blue; C, gray). Hydrogen atoms are omitted for clarity.

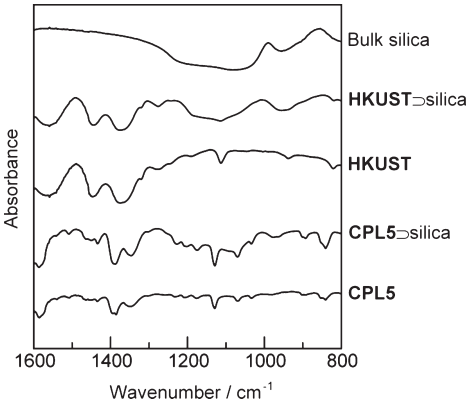

Figure 2. IR spectra of **HKUST**, **HKUST**⊃silica, **CPL5**, **CPL5**⊃silica, and bulk silica.

EXPERIMENTAL SECTION

Materials. All the reagents and chemicals used were obtained from commercial sources, unless otherwise noted. Tetramethoxysilane (TMOS) was purified by vacuum distillation prior to use. The host PCPs, $[Cu_3(btc)_2]_n$(**HKUST**) and $[Cu_2(pzdc)_2(dpe)]_n$ (**CPL5**), were prepared using methods reported previously.[2d,5,6]

Sol−Gel Synthesis of Silica in HKUST. The dried host compound **HKUST** (417 mg) was prepared by evacuation (<0.1 kPa) at 130 °C for 5 h in a Pyrex reaction tube. Subsequently, the host powder was immersed in 2 mL of TMOS at room temperature for 15 min under

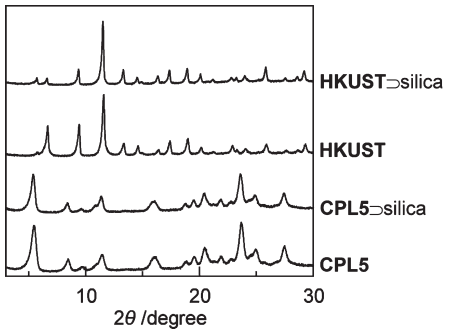

Figure 3. XRPD patterns of **HKUST**, **HKUST**⊃silica, **CPL5**, and **CPL5**⊃silica.

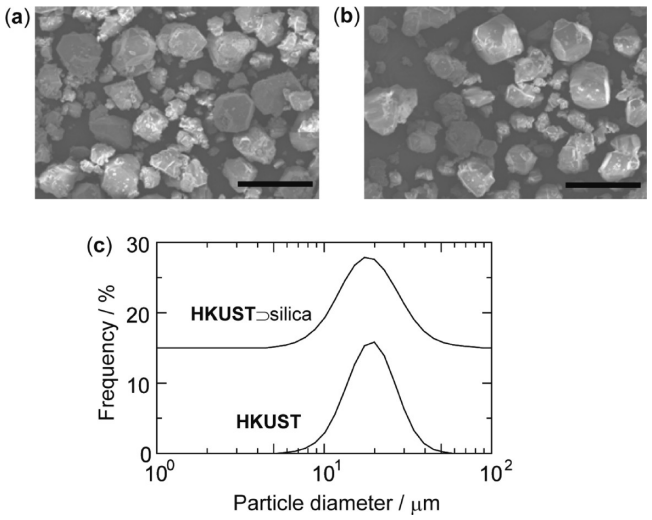

Figure 4. SEM images of (a) **HKUST** and (b) **HKUST**⊃silica (scale bar = 50 μm) and (c) their particle size distributions.

nitrogen atmosphere to incorporate TMOS into the nanochannels. Excess amount of TMOS external to the host crystals was removed completely by evacuation (50 Pa) at room temperature for 15 min to obtain **HKUST**-TMOS adduct (638 mg), the reaction tube was then left for 24 h under exposure to H_2O vapor, followed by heating at 60 °C for 24 h in air. For further condensation and removal of byproducts (water and methanol), the resultant composite was finally incubated at 110 °C for 24 h in vacuum to obtain **HKUST**-silica composites (**HKUST**⊃silica; 508 mg).

Measurements. The X-ray powder diffraction (XRPD) data were collected using a Rigaku RINT 2000 Ultima diffractometer employing CuKα radiation. The thermogravimetric (TG) analysis was carried out from room temperature to 500 °C using a Rigaku Instrument Thermo plus TG 8120 in a nitrogen atmosphere. The infrared spectra were measured using KBr disks employing a PerkinElemer Spectrum BX FT-IR system. Solid-state ^{29}Si NMR was measured by JEOL JNM-LA300WB spectrometer. Particle size distributions of dry powder samples were measured by HORIBA Partica LA-950 laser diffraction particle size analyzer. Scanning Electron Microscope (SEM) measurement was performed by use of a Hitachi S-3000N at an accelerating voltage of 5 kV. SEM energy-dispersive X-ray (EDX) measurements were conducted by using a JEOL JED-2300 detector in a JEOL JSM-5600 at an accelerating voltage of 15 kV. Nitrogen adsorption measurements at 77 K and solvent vapor adsorption measurements at 298 K were carried out using a Quantachrome Autosorb-1 and BELSORP-18,

dx.doi.org/10.1021/cm102610r |*Chem. Mater.* 2011, 23, 1736–1741

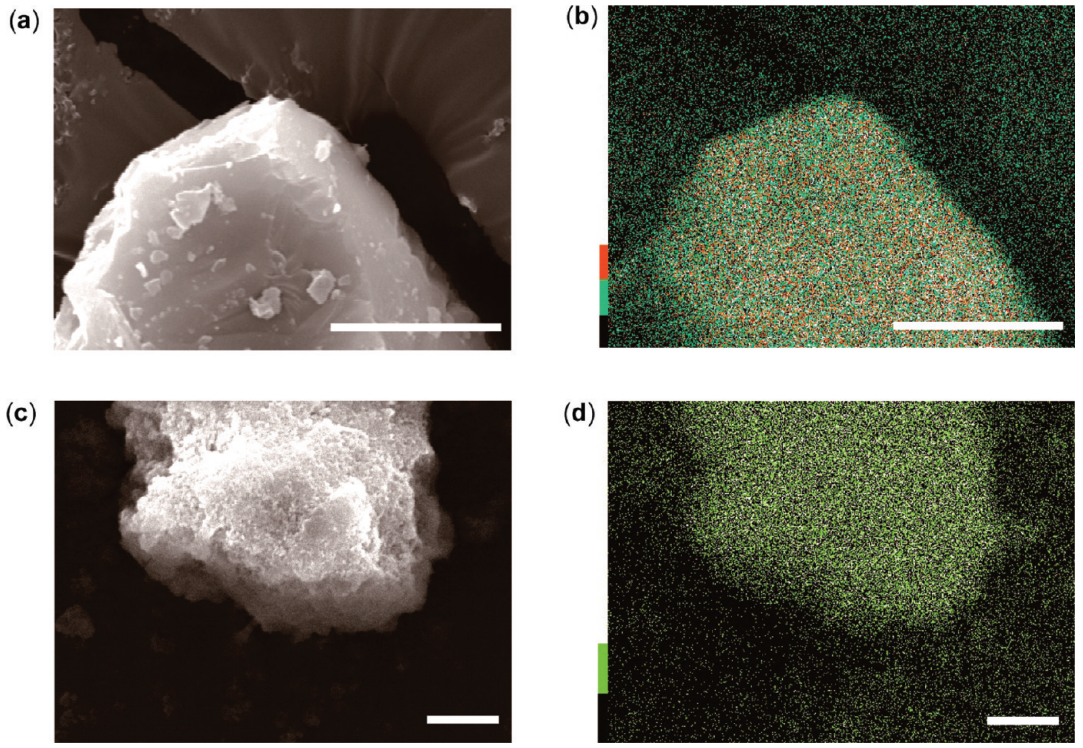

Figure 5. (a) SEM image and (b) SEM-EDX elemental (Si) map of **HKUST**⊃silica. (c) SEM image and (d) SEM-EDX elemental (Si) map of **CPL5**⊃silica. Scale bars = 5 μm.

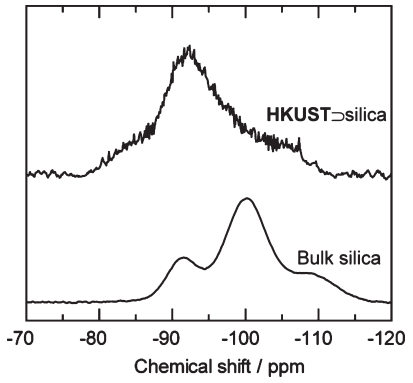

Figure 6. Solid-state ^{29}Si NMR spectra of **HKUST**⊃silica and bulk silica.

respectively. The samples were dried under high vacuum (<1 × 10^{-2} Pa) at 120 °C for 5 h before the measurements were performed.

RESULTS AND DISCUSSION

Preparation of Silica in the Pore of HKUST. According to the reported procedure using **CPL5**,[2d] we performed sol−gel reaction of TMOS in **HKUST** to deposit silica particles inside the channels. After the encapsulation of TMOS in the PCP channels, the encapsulated TMOS was hydrolyzed under H_2O vapor to produce reactive silanol species. Polycondensation reaction was induced by heating the materials to provide a host−guest nanocomposite (**HKUST**⊃silica). In this system, the channels of the host was fully filled with TMOS (weight of TMOS/weight of **HKUST** = 0.53), where one unit cell of **HKUST** could accommodate 2.1 TMOS molecules, before the reaction. However, loading amount of silica in **HKUST** was lower (weight of silica/weight of **HKUST** = 0.22) because of the removal of MeOH and water as byproducts in the polycondensation process. Hence, the host channels were not fully occupied with silica particles, suggesting that the **HKUST**⊃silica composite still have void spaces accessible to additional guest molecules. We conducted IR measurements to confirm the formation of silica in the host pore. In the IR spectra of **HKUST**⊃silica, a broad band assignable to Si−O stretching vibration from 1000 to 1250 cm^{-1} was clearly found in addition to the peaks for the original host (Figure 2).[7] In the XRPD measurements, peak pattern of **HKUST**⊃silica was almost the same to that of the only host, indicating the host channel framework was maintained during the sol−gel reaction (Figure 3). SEM measurement showed that the particle size, shape, and surface of the host crystals were not changed before and after the sol−gel reaction, which is consistent with the analysis of particle size distribution by laser light diffraction (Figure 4). We also carried out SEM-EDX elemental mapping measurements to confirm the distribution of silica particles in the host crystal (Figure 5). Elemental map for **HKUST**⊃silica showed homogeneous distribution of Si atoms in the crystal, indicating homogeneous dispersion of silica particle in the host channels. In addition, incorporation ratio of Si atom per unit cell of **HKUST** was found to be 1.9, which is consistent with the loading amount of TMOS in **HKUST**.

To understand the degree of silica condensation, ^{29}Si magic angle spinning (MAS) NMR measurement of **HKUST**⊃silica was performed (Figure 6).[8] A reference sample of bulk material, prepared under similar conditions, exhibits an intense peak for the Q^3 unit at −100 ppm, along with peaks assignable to Q^2 and Q^4 at −92 and −109 ppm, respectively (where

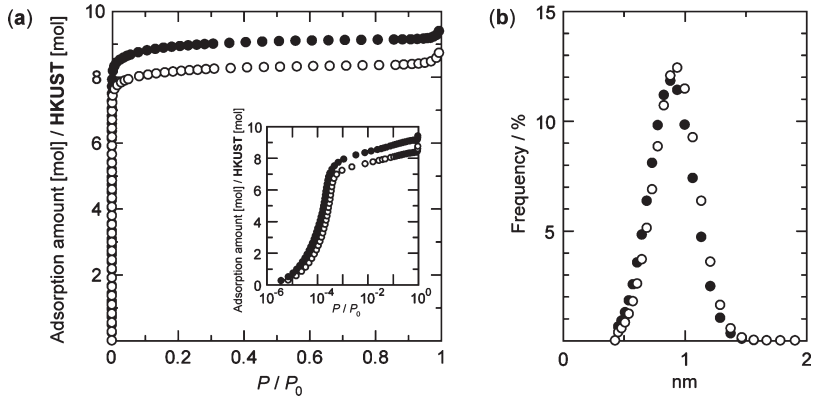

Figure 7. (a) N_2 adsorption isotherms for **HKUST** (●) and **HKUST**⊃silica (○) at 77 K. The inset shows the adsorption isotherms plotted against a logarithmic relative pressure. (b) Pore size distributions of **HKUST** (●) and **HKUST**⊃silica (○) using nonlocalized density functional theory, determined from N_2 adsorption profile.

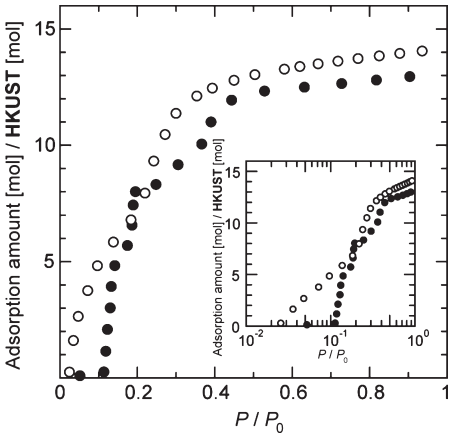

Figure 8. H_2O adsorption isotherms for **HKUST** (●) and **HKUST**⊃silica (○) at 298K. The inset shows the adsorption isotherms plotted against a logarithmic relative pressure.

$Q^n = Si(OSiX)_n(OH)_{4-n}$). Despite the relatively low resolution in the spectrum of **HKUST**⊃silica because of the existence of paramagnetic Cu^{2+} ions, this spectrum showed that the domain of Q^2 increases and the fully cross-linked Q^4 unit was hardly detectable compared with that of bulk silica. A shoulder peak corresponding to terminal moiety (Q^1) of silica is also observed around −83 ppm. These NMR results clearly indicate that the growth of silica is highly constrained in the narrow host channels, which was also seen in the case using **CPL5** as a host matrix. Formation of silica nanoparticles with constrained geometries leads to increase in hydrophilic silanol moiety on the particle surfaces.

Adsorption Properties of PCP−Silica Composites. We carried out nitrogen adsorption measurement for **HKUST**⊃silica at 77 K (Figure 7a). The adsorption isotherm showed a typical Type I profile,[9] suggesting that the micropores of the host are still accessible by nitrogen molecules. In comparison with the isotherm obtained from only **HKUST**, more than 80% of the micropore in **HKUST**⊃silica are available for further adsorption of guest molecules (Figure 7a). We also compared pore size distributions between **HKUST** and **HKUST**⊃silica, and found almost no difference before and after the formation of silica inside the pores of **HKUST** (Figure 7b). In addition, the adsorption of nitrogen molecules into the pores of

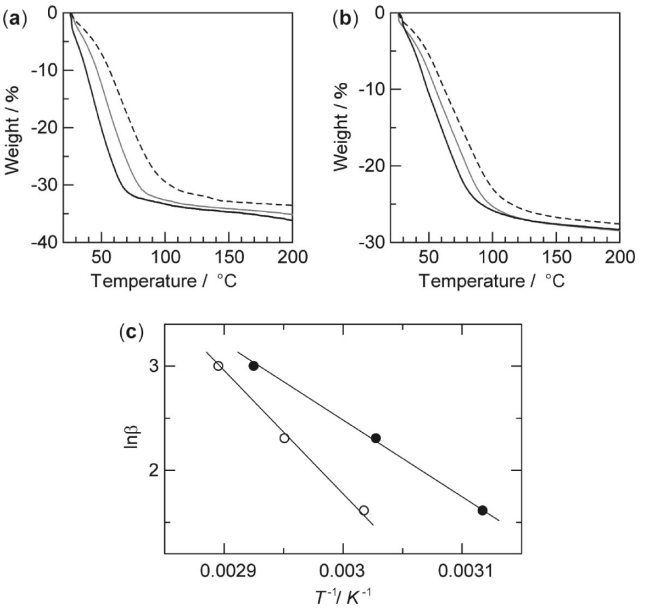

Figure 9. Water desorption TG curves of (a) **HKUST** and (b) **HKUST**⊃silica under a N_2 atmosphere. Heating rate; 5 K/min (black), 10 K/min (gray), and 20 K/min (dot). (c) Plots of logarithms of heating rate (β) versus reciprocal temperatures at 50% water desorption from **HKUST** (●) and **HKUST**⊃silica (○).

HKUST⊃silica starts at the similar pressure to that of the only host (Figure 7a inset). Thus these results exclude the possibility that the pore walls of **HKUST**⊃silica were homogeneously covered with thin silica, but indicate the dispersion of silica as small isolated nanoparticles in the pores.

To probe the hydrophilicity of **HKUST**⊃silica, we carried out the adsorption measurements of **HKUST** and **HKUST**⊃silica on water at 298 K. As shown in Figure 8, the adsorption of water in **HKUST**⊃silica started at a lower relative pressure compared with that in **HKUST**, showing the remarkable effect of silica on the adsorption of water (Figure 8 inset). The higher affinity of **HKUST**⊃silica to water should be caused by incarceration of hydrophilic silica inside the pores, enhancing the capability of the host for water storage. To evaluate the strong interaction between water and **HKUST**⊃silica, the activation energies (E)

dx.doi.org/10.1021/cm102610r |*Chem. Mater.* 2011, 23, 1736–1741

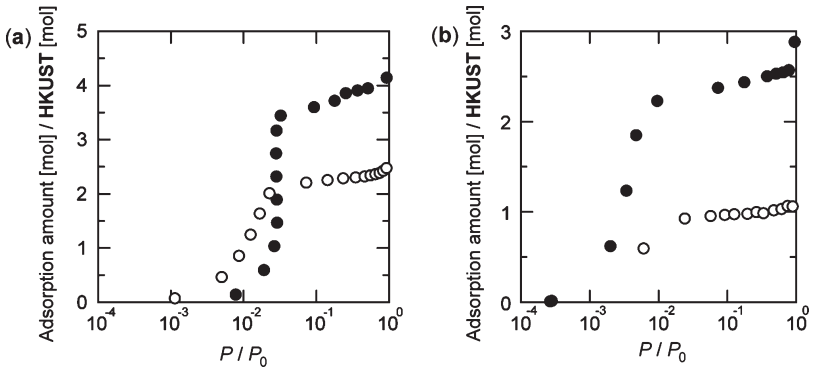

Figure 10. Adsorption isotherms plotted against a logarithmic relative pressure on (a) 1,4-dioxane and (b) cyclohexane at 298 K for **HKUST** (●) and **HKUST**⊃silica (○).

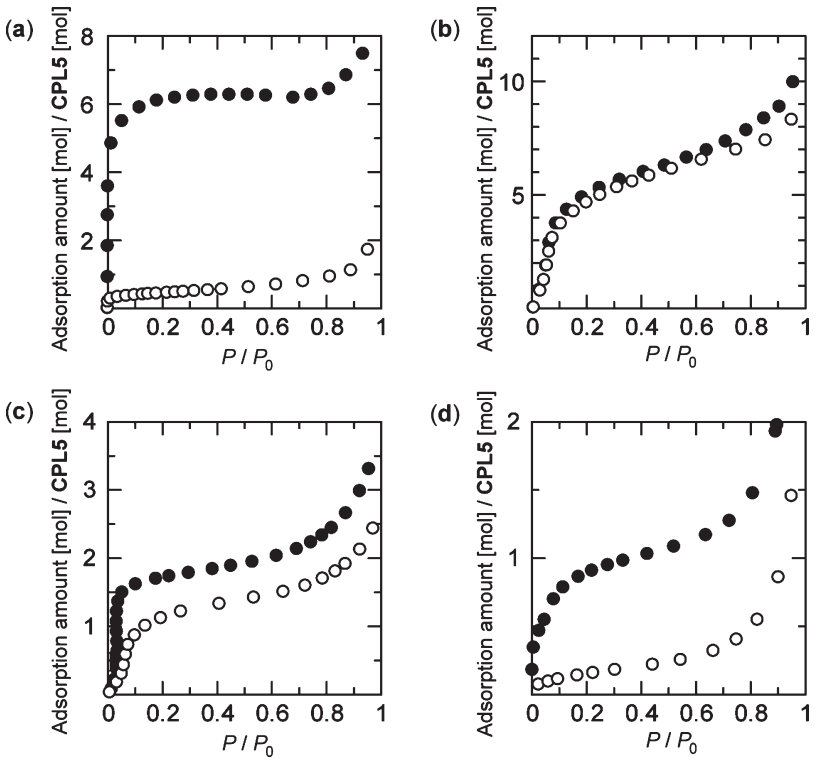

Figure 11. Adsorption isotherms of (a) N_2 at 77 K, (b) H_2O, (c) 1,4-dioxane, and (d) cyclohexane at 298 K for **CPL5** (●) and **CPL5**⊃silica (○).

of water desorption from **HKUST** or **HKUST**⊃silica were estimated by recording TG curves at various heating rates (β) as follows[10]

$$\ln \beta = -1.0516E/RT + \text{const}$$

where R is gas constant and T is temperature at 50% desorption of water. As is seen in panels a and b in Figure 9, values of T shift to higher temperatures with increasing β. Linear lines, which are obtained by plotting $\ln\beta$ vs T^{-1}, could determine E of **HKUST** and **HKUST**⊃silica as 63 and 99 kJ/mol, respectively (Figure 9c). These quantitative TG analyses could also support the strong affinity between water and **HKUST**⊃silica.

We performed the adsorption measurements on 1,4-dioxane and cyclohexane at 298 K to gain the insights into the adsorption property of **HKUST**⊃silica (Figure 10). Although the size of these molecules are comparable, the polarities of these solvents are quite different, showing the polarity parameters (P') of 1, 4-dioxane and cyclohexane as 5.8 and 0.2, respectively (e.g., P' of water =10.2, P′ of benzene =2.7).[11] Therefore 1,4-dioxane is soluble in water, but cyclohexane is not miscible with water. Because of the existence of silica inside the pore, the adsorption amounts of **HKUST**⊃silica for both solvents were found to decrease in comparison with those of only **HKUST**. However, **HKUST**⊃silica could start to adsorb 1,4-dioxane at lower relative pressure than **HKUST**, in contrast, the initial adsorption points for cyclohaxane in **HKUST** and **HKUST**⊃silica were almost the same. These results also indicate the affinity of **HKUST**⊃silica to hydrophilic molecules because of the incarceration of silica inside the pores.

CPL5 has one-dimensional channel structure and its pore size is similar to that of **HKUST**. Thus, formation of silica

dx.doi.org/10.1021/cm102610r |*Chem. Mater.* 2011, 23, 1736–1741

nanoparticles inside the channels of **CPL5** can allow us to study the effects of pore dimensionality on the adsorption properties of PCP−silica hybrids. We performed sol−gel synthesis of silica in the nanochannels of **CPL5** according to the reported method, and characterized the resulting composite (**CPL5**⊃silica) by XRPD, IR, and SEM-EDX measurements (Figures 2, 3, and 5).[2d] Formation of nanosized silica homogeneously distributed in the channels of **CPL5** was confirmed (weight of silica/weight of **CPL5**⊃silica = 0.11), where accessible void spaces are still remaining in the frameworks.

We performed nitrogen adsorption measurement of **CPL5**⊃silica at 77 K, which showed almost no adsorption property (Figure 11a). This interesting fact means that nitrogen molecules cannot diffuse into the pores of **CPL5** because of the blocking effect of silica nanoparticles accommodated in the one-dimensional channels. In contrast, water molecules could be highly adsorbed into the pores of **CPL5**⊃silica at 298 K, and the adsorption amount was comparable to that in only host (Figure 11b). Similarly to the **HKUST** system, modification of **CPL5** pores with hydrophilic silica can enhance the adsorption property for water. In addition, adsorption behaviors of **CPL5**⊃silica on 1,4-dioxane and cyclohexane exhibited clear difference, where 1,4-dioxane was efficiently adsorbed at the lower pressure region but diffusion of cyclohexane was highly restricted (Figure 11c, d). Compared to the **HKUST** system, the effect of silica modification on the adsorption for these solvent molecules was found to be more evident in **CPL5**⊃silica. As the sizes of pores in **HKUST** and **CPL5** are the almost similar, the dimensionality of these PCPs would critically affect the adsorption properties of the silica composites. In case of **HKUST**⊃silica, guest molecules can diffuse throughout the channels of **HKUST** because of its interconnecting three-dimensional porous structures. However, guest molecules must pass through the silica-modified channels to be adsorbed in **CPL5**⊃silica with one-dimensional porous system, resulting in significant gate effect on selectivity for the adsorbates.[12]

CONCLUSIONS

We have performed sol−gel synthesis of silica in **HKUST** and **CPL5** to incarcerate silica nanoparticles into the nanochannels. Modification of these PCP pores with silica particles could allow the selective adsorption for hydrophilic molecules, where this effect are remarkably enhanced in one-dimensional channels of **CPL5** rather than in three-dimensional interconnecting pores of **HKUST**. We believe that this methodology will contribute to the development of PCPs for their application as unique storage and separation materials. Because a variety of inorganic metal oxides can be prepared by sol−gel process, infinite combinations between PCPs and metal oxide nanoparticles can lead to design or tune the porous properties of PCP materials.

AUTHOR INFORMATION

Corresponding Author

*E-mail: uemura@sbchem.kyoto-u.ac.jp, kitagawa@icems.kyoto-u.ac.jp.

ACKNOWLEDGMENT

We thank Prof. Y. Chujo of Kyoto University for access to SEM-EDX apparatuses. This work was supported by PRESTO-JST and a Grant-in-Aid from the Ministry of Education, Culture, Sports, Science and Technology, Government of Japan.

REFERENCES

(1) For selected reviews on PCPs, see: (a) Yaghi, O. M.; Li, H. L.; Davis, C.; Richardson, D.; Groy, T. L. *Acc. Chem. Res.* **1998**, *31*, 474. (b) Moulton, B.; Zaworotko, M. J. *Chem. Rev.* **2001**, *101*, 1629. (c) Férey, G. *Chem. Soc. Rev.* **2008**, *37*, 191. (d) Kitagawa, S.; Kitaura, R.; Noro, S.-i. *Angew. Chem., Int. Ed.* **2004**, *43*, 2334. (e) Corma, A.; Garcia, H.; Llabrés i Xamena, F. X. *Chem. Rev.* **2010**, *110*, 4606. (f) Côté, A. P.; Shimizu, G. K. H. *Coord. Chem. Rev.* **2003**, *245*, 49. (g) Bradshaw, D.; Claridge, J. B.; Cussen, E. J.; Prior, T. J.; Rosseinsky, M. J. *Acc. Chem. Res.* **2005**, *38*, 273. (h) Maspoch, D.; Ruiz-Molina, D.; Veciana, J. *Chem. Soc. Rev.* **2007**, *36*, 770.

(2) (a) Hermes, S.; Schröter, M.-K.; Schmid, R.; Khodeir, L.; Muhler, M.; Tissler, A.; Fischer, R. W.; Fischer, R. A. *Angew. Chem., Int. Ed.* **2005**, *44*, 6237. (b) Schröder, F.; Esken, D.; Cokoja, M.; van den Berg, M. W. E.; Lebedev, O. I.; Van Tendeloo, G.; Walaszek, B.; Buntkowsky, G.; Limbach, H.-H.; Chaudret, B.; Fischer, R. A. *J. Am. Chem. Soc.* **2008**, *130*, 6119. (c) Müller, M.; Zhang, X.; Wang, Y.; Fischer, R. A. *Chem. Commun.* **2009**, 119. (d) Uemura, T.; Hiramatsu, D.; Yoshida, K.; Isoda, S.; Kitagawa, S. *J. Am. Chem. Soc.* **2008**, *130*, 9216. (e) Hwang, Y. K.; Hong, D.-Y.; Chang, J.-S.; Jhung, S. H.; Seo, Y.-K.; Kim, J.; Vimont, A.; Daturi, M.; Serre, C.; Férey, G. *Angew. Chem., Int. Ed.* **2008**, *47*, 4144. (f) Zlotea, C.; Campesi, R.; Cuevas, F.; Leroy, E.; Dibandjo, P.; Volkringer, C.; Loiseau, T.; Férey, G.; Latroche, M. *J. Am. Chem. Soc.* **2010**, *132*, 2991. (g) Moon, H. R.; Kim, J. H.; Suh, M. P. *Angew. Chem., Int. Ed.* **2005**, *44*, 1261. (h) Sabo, M.; Henschel, A.; Fröde, H.; Klemm, E.; Kaskel, S. *J. Mater. Chem.* **2007**, *17*, 3827.

(3) (a) Halas, N. J. *ACS Nano* **2008**, *2*, 179. (b) Shenhar, R.; Rotello, V. M. *Acc. Chem. Res.* **2003**, *36*, 549. (c) Caruso, R. A.; Antonietti, M. *Chem. Mater.* **2001**, *13*, 3272.

(4) (a) Gambino, G. L.; Grassi, A.; Marletta, G. *J. Phys. Chem. B* **2006**, *110*, 4836. (b) Asay, D. B.; Barnette, A. L.; Kim, S. H. *J. Phys. Chem. C* **2009**, *113*, 2128. (c) Rodriguez, J.; Elola, M. D.; Laria, D. *J. Phys. Chem. B* **2009**, *113*, 12744.

(5) Uemura, T.; Kitaura, R.; Ohta, Y.; Nagaoka, M.; Kitagawa, S. *Angew. Chem., Int. Ed.* **2006**, *45*, 4112.

(6) (a) Chui, S. S.-Y.; Lo, S. M.-F.; Charmant, J. P. H.; Orpen, A. G.; Williams, I. D. *Science* **1999**, *283*, 1148. (b) Schlichte, K.; Kratzke, T.; Kaskel, S. *Microporous Mesoporous Mater.* **2004**, *73*, 81. (c) Alaerts, L.; Séguin, E.; Poelman, H.; Thibault-Starzyk, F.; Jacobs, P. A.; De Vos, D. E. *Chem.—Eur. J.* **2006**, *12*, 7353.

(7) (a) Ishii, M.; Shimanouchi, T.; Nakahira, M. *Inorg. Chim. Acta* **1967**, *1*, 387. (b) Farmer, V. C. *The Infrared Spectra of Minerals*; Farmer, V. C., Ed.; Mineral Society: London, 1974; p 331.

(8) Englehardt, G.; Michel, D. *High-Resolution Solid-State NMR of Silicate and Zeolites*; Wiley: New York, 1987; pp 75.

(9) Brunauer, S.; Deming, L. S.; Deming, W. E.; Teller, E. *J. Am. Chem. Soc.* **1940**, *62*, 1723.

(10) (a) Uemura, K.; Kitagawa, S.; Fukui, S.; Saito, K. *J. Am. Chem. Soc.* **2004**, *126*, 3817. (b) Flynn, J. H.; Wall, L. A. *J. Polym. Sci., Part B* **1966**, *4*, 323.

(11) Snyder, L. R. *J. Chromatogr. Sci.* **1978**, *16*, 223.

(12) (a) Martin, C.; Tosi-Pellenq, N.; Patarin, J.; Coulomb, J. P. *Langmuir* **1998**, *14*, 1774. (b) Cracknell, R. F.; Gubbins, K. E. *Langmuir* **1993**, *9*, 824.